

Mechanistic investigation of a highly active phosphite dehydrogenase mutant and its application for NADPH regeneration

Ryan Woodyer¹, Huimin Zhao² and Wilfred A van der Donk^{1,3}

¹ Department of Chemistry, University of Illinois at Urbana-Champaign, Urbana, IL, USA

² Department of Chemical and Biomolecular Engineering, University of Illinois at Urbana-Champaign, Urbana, IL, USA

³ Department of Biochemistry, University of Illinois at Urbana-Champaign, Urbana, IL, USA

Keywords

biocatalysis; cofactor regeneration; dehydrogenases; homology modelling; site-directed mutagenesis

Correspondence

H. Zhao, Department of Chemical and Biomolecular Engineering, University of Illinois at Urbana-Champaign, 600 S. Mathews Ave, IL 61801, USA

Fax: +1 217 3335052

Tel: +1 217 3332631

E-mail: zhao5@uiuc.edu

W. A. van der Donk

Department of Chemistry, 600 S. Mathews Ave, IL 61801, USA

Fax: +1 217 2448024

Tel: +1 217 2445360

E-mail: vdndonk@uiuc.edu

(Received 5 March 2005, revised 14 April 2005, accepted 23 May 2005)

doi:10.1111/j.1742-4658.2005.04788.x

NAD(P)H regeneration is important for biocatalytic reactions that require these costly cofactors. A mutant phosphite dehydrogenase (PTDH-E175A/A176R) that utilizes both NAD and NADP efficiently is a very promising system for NAD(P)H regeneration. In this work, both the kinetic mechanism and practical application of PTDH-E175A/A176R were investigated for better understanding of the enzyme and to provide a basis for future optimization. Kinetic isotope effect studies with PTDH-E175A/A176R showed that the hydride transfer step is (partially) rate determining with both NAD and NADP giving $^D V$ values of 2.2 and 1.7, respectively, and $^D V/K_{m,\text{phosphite}}$ values of 1.9 and 1.7, respectively. To better comprehend the relaxed cofactor specificity, the cofactor dissociation constants were determined utilizing tryptophan intrinsic fluorescence quenching. The dissociation constants of NAD and NADP with PTDH-E175A/A176R were 53 and 1.9 μM , respectively, while those of the products NADH and NADPH were 17.4 and 1.22 μM , respectively. Using sulfite as a substrate mimic, the binding order was established, with the cofactor binding first and sulfite binding second. The low dissociation constant for the cofactor product NADPH combined with the reduced values for $^D V$ and k_{cat} implies that product release may become partially rate determining. However, product inhibition does not prevent efficient *in situ* NADPH regeneration by PTDH-E175A/A176R in a model system in which xylose was converted into xylitol by NADP-dependent xylose reductase. The *in situ* regeneration proceeded at a rate approximately fourfold faster with PTDH-E175A/A176R than with either WT PTDH or a NADP-specific *Pseudomonas* sp.101 formate dehydrogenase mutant with a total turnover number for NADPH of 2500.

The use of enzymes as catalysts in industrial and academic processes has become increasingly important over the past few decades [1–6]. One of the barriers to widespread implementation of biocatalytic processes

has been the feasibility of complex biocatalytic transformations on the industrial scale [7]. Such reactions usually require cofactors that are too expensive to be added in stoichiometric amounts for large-scale

Abbreviations

DH, dehydrogenases; FDH, formate dehydrogenase; FPLC, fast performance liquid chromatography; IPTG, isopropyl- β -D-thiogalactopyranoside; IMAC, immobilized metal affinity chromatography; KIE, kinetic isotope effect; NAD⁺, NADH, nicotinamide adenine dinucleotide; NADP⁺, NADPH, nicotinamide adenine dinucleotide phosphate; Pt-H, phosphite; PTDH, phosphite dehydrogenase; $^D V$, kinetic isotope effect on V_{max} ; $^D V/K$, kinetic isotope effect on V_{max}/K_m ; WT, wild-type; XR, xylose reductase.

processes [8–10]. Two primary solutions to this problem have been devised; either the reaction is performed with whole cells using the cellular supply of cofactors, or the cofactors are regenerated *in situ* using a sacrificial substrate. Several reviews discuss the available methods and benefits of regeneration of a number of cofactors [8,9,11,12].

NAD(P)H is involved in approximately 80% of enzymatic reductions accounting for over 300 known reactions, many of which have potential in biocatalysis [13]. As a result, several regeneration systems for NAD(P)H have been described that allow cofactor addition in catalytic amounts [9,14–16]. Of these, enzymatic methods are currently the most attractive as they have shown high turnover number and relatively low cost. The most widely used NADH regenerative enzymes are formate dehydrogenases (FDH) from *Pseudomonas* sp.101 [17] and *Candida boidinii* [18,19], the latter of which is used in the industrial production of L-*tert*-leucine [19]. Regenerative methods exist for NADPH as well, including the use of glucose dehydrogenase (GDH) and the use of a mutant FDH from *Pseudomonas* sp.101 (mut-Pse FDH). However, both NADPH regeneration systems suffer from various disadvantages such as strong product inhibition (GDH), high K_m values (GDH and FDH), high enzyme cost (GDH and FDH) and low catalytic activity (FDH) [11,12]. Due to this lack of an efficient system, NADPH regeneration has not been applied in large-scale syntheses.

The cofactors NAD and NADP are ubiquitous and differ only by the 2'-phosphate group that is attached to the adenine ribose in NADP. Nature has exploited this difference by evolving enzymes that have very high selectivity for one cofactor over the other. This selectivity is important for proper cellular function, as in Nature NAD is used almost exclusively for oxidative degradations that eventually lead to production of ATP, whereas NADP is typically utilized as a reductant in biosynthetic reactions with few exceptions [20]. Therefore, the *potential* of NADPH regeneration for

biosynthetic applications may be greater than that of NADH regeneration. Currently, NADH-dependent enzymes are employed most frequently due to the expense of NADPH and the lack of a good regeneration system. Hence the development of an efficient NADPH regeneration system is highly desired.

Phosphite dehydrogenase (PTDH) [21] is a promising NADH regeneration catalyst that fulfills many of the criteria for efficient cofactor recycling systems such as a low cost innocuous sacrificial substrate with a low K_m value [22]. However, the wild-type (WT) enzyme utilizes NADP poorly, limiting its use to NADH regeneration. In a recent study, a rational design approach was used for the generation of a mutant PTDH (E175A, A176R) that accepts NADP with high catalytic efficiency while maintaining high activity with NAD [23]. In this mutant, an Ala replaced Glu175, which makes hydrogen-bonding contacts to the 2'- and 3'-hydroxyl groups of the adenine ribose moiety of NAD in WT PTDH, and an Arg replaced Ala176 to stabilize the additional negative charge of NADP. PTDH-E175A/A176R displayed relaxed cofactor specificity with a K_m for NADP that is decreased over 700-fold compared with the WT enzyme (Table 1) and that displays high catalytic efficiency with both NAD and NADP. The resulting kinetics compare favorably with the best FDH NADPH regeneration enzymes (Table 1).

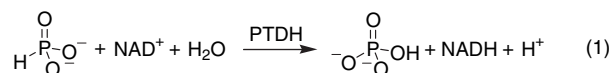
Changing cofactor specificity of oxidoreductases has been achieved before, but very few examples exist where catalytic efficiency for the noncanonical cofactor has been improved to approximately that for the canonical substrate [24–32]. Even fewer are the examples where specificity becomes relaxed allowing high catalytic efficiency with both NAD(H) and NADP(H) [25,26,28,31]. Thus PTDH-E175A/A176R, with its relaxed cofactor specificity, is interesting from the standpoint of protein engineering and very promising with respect to cofactor regeneration. Here we show the enzyme's efficacy at *in situ* NADPH regeneration

Table 1. Kinetic comparison of WT and Mutant PTDH and FDH with either NADP or NAD.

Enzyme (cofactor)	K_M NADP (μM)	k_{cat} (min^{-1})	k_{cat}/K_M , NADP ($\mu\text{M}^{-1}\cdot\text{min}^{-1}$)	K_M (μM , Pt-H or formate)
WT PTDH (NAD) ^a	53 ± 9.0	176 ± 8	3.3	47 ± 6.0
WT PTDH (NADP) ^a	2510 ± 410	84.6 ± 0.5	0.0337	1880 ± 325
E175A/A176R (NAD) ^a	20 ± 1.3	236.4 ± 0.5	11.8	61 ± 13
E175A/A176R (NADP) ^a	3.5 ± 0.5	114 ± 33	32.6	21 ± 2.7
WT FDH (NAD) ^b	60 ± 5	600 ± 36	10	7000 ± 800
WT FDH (NADP) ^b	> 400 000	ND ^c	ND	ND
Mut. FDH (NAD) ^b	1000 ± 150	300 ± 24	0.3	9000 ± 3000
Mut. FDH (NADP) ^b	150 ± 25, 290 ^d	150 ± 9	1, 0.5 ^d	9000 ± 3000

^a Performed at 25 °C [23]; ^b performed at 30 °C [47]; ^c none detected; ^d reported by Juelich Fine Chemicals.

using a recently discovered highly efficient NADPH-dependent xylose reductase [33] as a model biocatalytic enzyme. Furthermore, from a basic biochemical perspective, PTDH-E175A/A176R may provide important insights into the mechanism of the reaction, which is a highly unusual phosphoryl transfer from a hydride donor to a hydroxide acceptor (Scheme 1) [34]. Thus, we also present a parallel study of the WT and PTDH-E175A/A176R enzymes with respect to kinetic isotope effects, product inhibition, and cofactor binding.



Results and Discussion

Kinetic isotope effects (KIEs)

Primary deuterium kinetic isotope effects (KIEs) were determined for V_{\max} ($^{\text{D}}V$), V/K_{NADP} ($^{\text{D}}V/K_{\text{m,NADP}}$), and V/K_{Pt} ($^{\text{D}}V/K_{\text{m,Pt}}$) by comparing the initial velocity patterns obtained with either phosphite (Pt) or deuterium labeled phosphite (Pt-D) in the reduction of NADP. This is the only direction in which PTDH can be assayed as the equilibrium constant is 10^{11} in favor of phosphate and NADH [22]. The reaction was monitored by varying the concentration of NAD (Fig. 1A) or NADP (Fig. 1B) at saturating concentrations of Pt or Pt-D, as well as by varying Pt or Pt-D concentrations at saturating NADP concentrations (data not shown). The kinetic parameters of each data set were obtained from fitting the data to the Michaelis–Menten equation providing $^{\text{D}}V$ and $^{\text{D}}V/K$ for both substrates as presented in Table 2.

The $^{\text{D}}V$ value for PTDH-E175A/A176R was 2.21 ± 0.03 with NAD and 1.7 ± 0.1 with NADP. Therefore, the hydride transfer step for the PTDH-E175A/A176R with both NAD and NADP is either (partially) rate determining, or it becomes rate determining with labeled phosphite. It is important to note that these isotope effects are larger than they appear at first glance, as the theoretical maximum for a classical KIE on the cleavage of P–H/P–D bonds in phosphite is approximately 5.0 at 25 °C, as estimated from previously reported stretching frequencies of these bonds [35]. $^{\text{D}}V$ for PTDH-E175A/A176R with NADP is significantly decreased compared with the reaction of the WT or PTDH-E175A/A176R enzymes with NAD. Taken together with the observation that k_{cat} is smaller with NADP as cofactor (Table 1), this finding suggests that a step other than hydride transfer is becoming more rate determining. The $^{\text{D}}V$ for PTDH-E175A/A176R

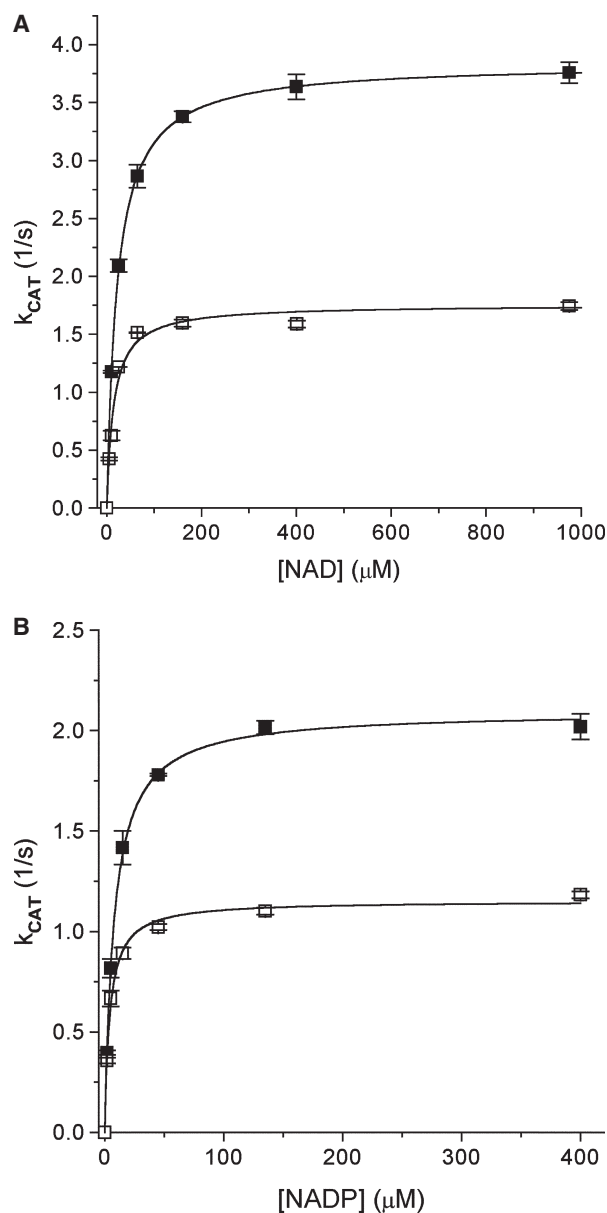


Fig. 1. Primary kinetic isotope effect of PTDH-E175A/A176R varying NAD concentration (A) or NAD(P) concentration (B). Deuterium labeled phosphite (\square) was prepared as outlined in Experimental procedures and compared with unlabeled phosphite (\blacksquare) for the enzymatic reduction of NADP. Phosphite concentrations (labeled or unlabeled) were held at 2 mM and the assay was started by the addition of 2 μg of His₆-tagged PTDH in each assay. The data was analyzed (Table 2) by fitting to the Michaelis–Menten equation.

with NAD (2.21) is similar to the $^{\text{D}}V$ KIE for the reaction of WT with NAD (2.1) [36] suggesting that the kinetic contribution of the hydride transfer step to the overall rate is similar for the mutant and WT PTDH when NAD is the cofactor. Given the strong thermodynamic driving force for the reaction, estima-

Table 2. Kinetic isotope effect with deuterated phosphite.

Enzyme (cofactor)	KIE $^D V$	$^D V/K_{\text{NADP}}$	$^D V/K_{\text{Phosphite}}$
WT (NAD) ^b	2.1 ± 0.1	1.0 ± 0.2	1.8 ± 0.3
E175A/A176R (NAD)	2.21 ± 0.03 ^a	1.4 ± 0.2	1.9 ± 0.1
E175A/A176R (NADP)	1.7 ± 0.1 ^a	1.0 ± 0.1	1.7 ± 0.2

^a Average of the values obtained. ^b Previously reported [36].

ted from redox potentials to be $\Delta G^0 = -15.1 \text{ kcal}\cdot\text{mol}^{-1}$ [22,36], it is interesting that the hydride transfer is rate determining at all.

$^D V/K_{\text{NAD}}$ for PTDH-E175A/A176R (1.4 ± 0.2) is close to the value of 1.0 ± 0.1 for this mutant with NADP ($^D V/K_{\text{NADP}}$). The slightly higher value for NAD (Table 2), may reflect that PTDH-E175A/A176R is not strictly ordered with respect to substrate binding because if NAD is the compulsory first substrate to bind, $^D V/K$ for the first substrate should be 1.0 [37–39]. Other examples exist where dehydrogenases are preferentially, but not completely ordered (e.g. D-xylitol dehydrogenase [40]). Finally, the $^D V/K_{\text{Pt}}$ values for PTDH-E175A/A176R were close to those for the WT enzyme for both cofactors (Table 2).

The relatively small $^D V$ KIE of PTDH-E175A/A176R is advantageous for the preparation of deuterated NADH or NADPH, which can subsequently be used in biocatalytic reactions to prepare stereospecifically labeled substrates in high isotopic purity as previously discussed for WT PTDH [22]. Combined with the fact that deuterated or tritiated phosphite is simple to prepare at low cost from D_2O ($^3\text{H}_2\text{O}$) and phosphorous acid [$\approx 35 \text{ USD}$ (\$) per kg, Aldrich 2004], this procedure may allow process scale production of high value stereospecifically labeled products.

Determination of dissociation constants by fluorescence quenching

The affinity of a cofactor regeneration enzyme for its cofactor substrate and product is an important parameter. Therefore, the dissociation constants (K_{D}) for the cofactor substrates and products were determined. WT and PTDH-E175A/A176R both have four tryptophan residues per monomer, but their positions are not established three-dimensionally because crystallographic information is currently not available. A homology model of WT-PTDH was constructed in previous work based on crystal structures of the sequence-related enzymes ($\approx 25\text{--}30\%$) D-lactate dehydrogenase, 3-phosphoglycerate dehydrogenase, and D-glycerate dehydrogenase [23]. This homology model was used to estimate the locations of these tryptophans with

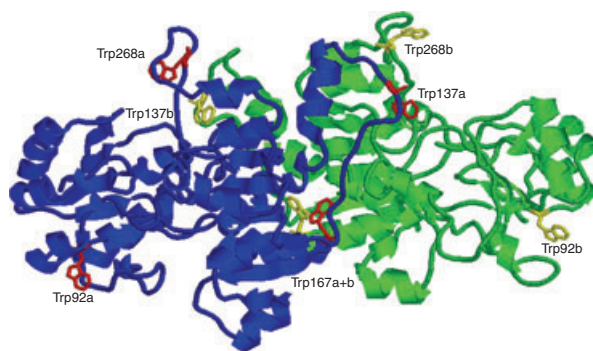


Fig. 2. Homology model of WT PTDH. The homodimer model is colored blue and green for monomers A and B, respectively. Tryptophan residues on monomer A are colored red, while tryptophan residues on monomer B are yellow. Trp137 and Trp268 are both located near the active site, while Trp92 is isolated from the active site and Trp167 is located at the dimerization interface.

respect to the PTDH dimer. Figure 2 shows that two of these tryptophans (Trp137 and Trp268) are located on flexible loops very close to the active site. Of the remaining two, Trp92 is solvent exposed and isolated from the active site while Trp167 is buried in the dimerization interface. The fluorescence properties of tryptophan vary significantly based on its local environment, which has been used in numerous studies to measure conformational changes in proteins, including those related to small molecule binding [41–49]. From Fig. 2 it appears that Trp137 and Trp268 provide a good spectroscopic handle to monitor substrate binding because they are close to the active site and their local environments are likely to change upon substrate binding based on the open and closed structures of other dehydrogenases.

PTDH-E175A/A176R provided a large fluorescence signal from 310 to 380 nm when excited at 295 nm at concentrations as low as $0.25 \mu\text{M}$ (dimer). When titrated with substrates or products, the fluorescence signal decreased significantly, showing saturation behavior (Fig. 3) and when plotted against concentration of titrant, single phase binding behavior was observed (Fig. 4). The data was fitted to Eqn 2 (Experimental procedures) to obtain K_{D} values assuming that all binding sites are occupied at the maximal change in fluorescence (ΔF_{max}). Figure 4 shows the binding curves for PTDH-E175A/A176R with NAD, NADH, NADP, and NADPH with the K_{D} values obtained displayed in Table 3. The data shows that PTDH-E175A/A176R binds both NADP and NADPH very tightly with K_{D} values of 1.9 and $1.22 \mu\text{M}$, respectively. The tight binding of NADP will allow low concentrations of cofactor to be used for *in situ* regeneration;

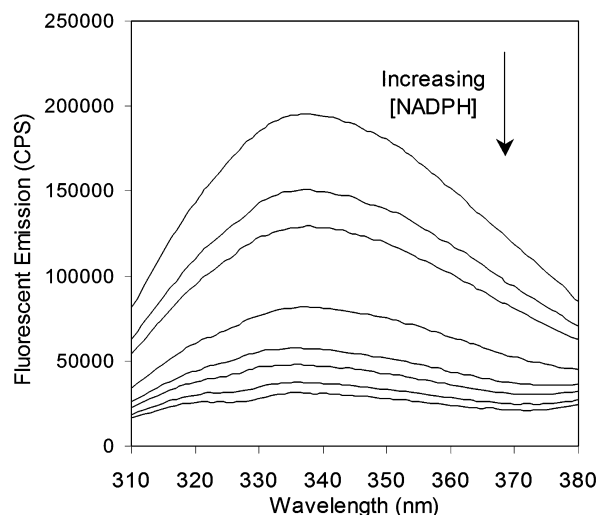


Fig. 3. Fluorescence emission spectrum of 0.25 μM PTDH-E175A/A176R at increasing NADPH concentrations. The intrinsic tryptophan fluorescence was observed by excitation at 295 nm and measuring the emission from 310 to 380 nm. NADPH was titrated into the sample to obtain final concentrations of 0, 0.5, 1, 2.9, 8.7, 17.4, 34.6, and 64 μM as described in the Experimental procedures.

however, the even tighter binding of NADPH suggested product inhibition might be a problem (*vide infra*). It is also obvious from the data that PTDH-E175A/A176R's affinity for NAD has decreased about fivefold as a result of the two mutations (Table 3). Previously, using the K_m values as estimates of dissociation constants, it was unclear as to what effect the mutations had on NAD binding (Table 1) [23]. The higher stability of the complex of WT PTDH and NAD is most likely due to the contributions of the hydrogen bonds between Glu175 and the 2'- and 3'-hydroxyl groups of the adenine ribose of NAD that are lost in PTDH-E175A/A176R. The binding site of PTDH-E175A/A176R has higher affinity for the reduced form of both cofactors compared with the oxidized forms (Table 3), which is the opposite of WT PTDH, suggesting PTDH-E175A/A176R is not as well adapted to the forward reaction of cofactor reduction as the WT enzyme.

Binding order of the substrates

Sulfite inhibits WT PTDH competitively with respect to phosphite and uncompetitively with respect to NAD [21]. It has a trigonal pyramidal shape with a lone pair on sulfur and resembles phosphite, which carries a proton on that lone pair. Therefore it is likely that sulfite occupies the same binding site as phosphite. As no catalytic turnover occurs, sulfite was utilized to

obtain additional information about binding order of substrates. Fluorescence was measured at varying sulfite concentrations (50 μM to 4 mM). These titration curves displayed only small changes in fluorescence ($\Delta F_{\text{max}} = 20\%$) at millimolar concentrations of sulfite and were not significantly different from control titrations with phosphate and sulfate. Neither sulfate nor phosphate inhibit WT PTDH to any substantial degree [21] at concentrations as high as 200 mM for phosphate [22], and therefore it is unlikely that the enzyme binds these anions in the phosphite binding site. Thus, the small changes in fluorescence observed during addition of sulfite are attributed to increased ionic strength and nonspecific binding. On the other hand, when PTDH-E175A/A176R was first incubated with saturating amounts of NAD (0.3 mM) or NADP (0.1 mM), titration with sulfite caused a large change in fluorescence ($\Delta F_{\text{max}} > 60\%$) displayed at concentrations of sulfite as low as 0.45 μM . K_D values of 1.00 ± 0.05 and 0.60 ± 0.06 μM were obtained in the presence of NAD and NADP, respectively (Table 4). These values are similar to the value determined for sulfite and WT PTDH in the presence of 0.2 mM NAD (0.76 ± 0.04 μM). The observed fluorescence changes in the presence of either cofactor show that sulfite forms a very stable ternary complex that causes a significant conformational change. In fact, a previous study has provided evidence that in this complex a covalent bond is formed between the sulfur of sulfite and C4 of NAD [50].

Using the same protocol, the binding of the cofactors was measured in the presence and absence of 0.2 mM sulfite as depicted in Fig. 5. NAD binds much tighter to PTDH-E175A/A176R in the presence of sulfite than in its absence. The same holds true for PTDH-E175A/A176R with NADP, where in the presence of sulfite the K_D drops from 1.9 μM (without sulfite) to a value too low to determine accurately with this method (< 0.5 μM). Collectively, the fluorescence experiments show that the cofactors can bind in the absence of sulfite, but sulfite does not bind with any significance in the absence of cofactor. This conclusion is consistent with the steady-state ordered mechanism with NAD binding first deduced from kinetic experiments for WT PTDH [21].

Product inhibition

Given the tight binding of the enzyme to NADPH, product release might be partially rate determining in PTDH-E175A/A176R. This supposition is supported by a k_{cat} with NADP that is smaller than that with NAD and furthermore by the partial masking of the

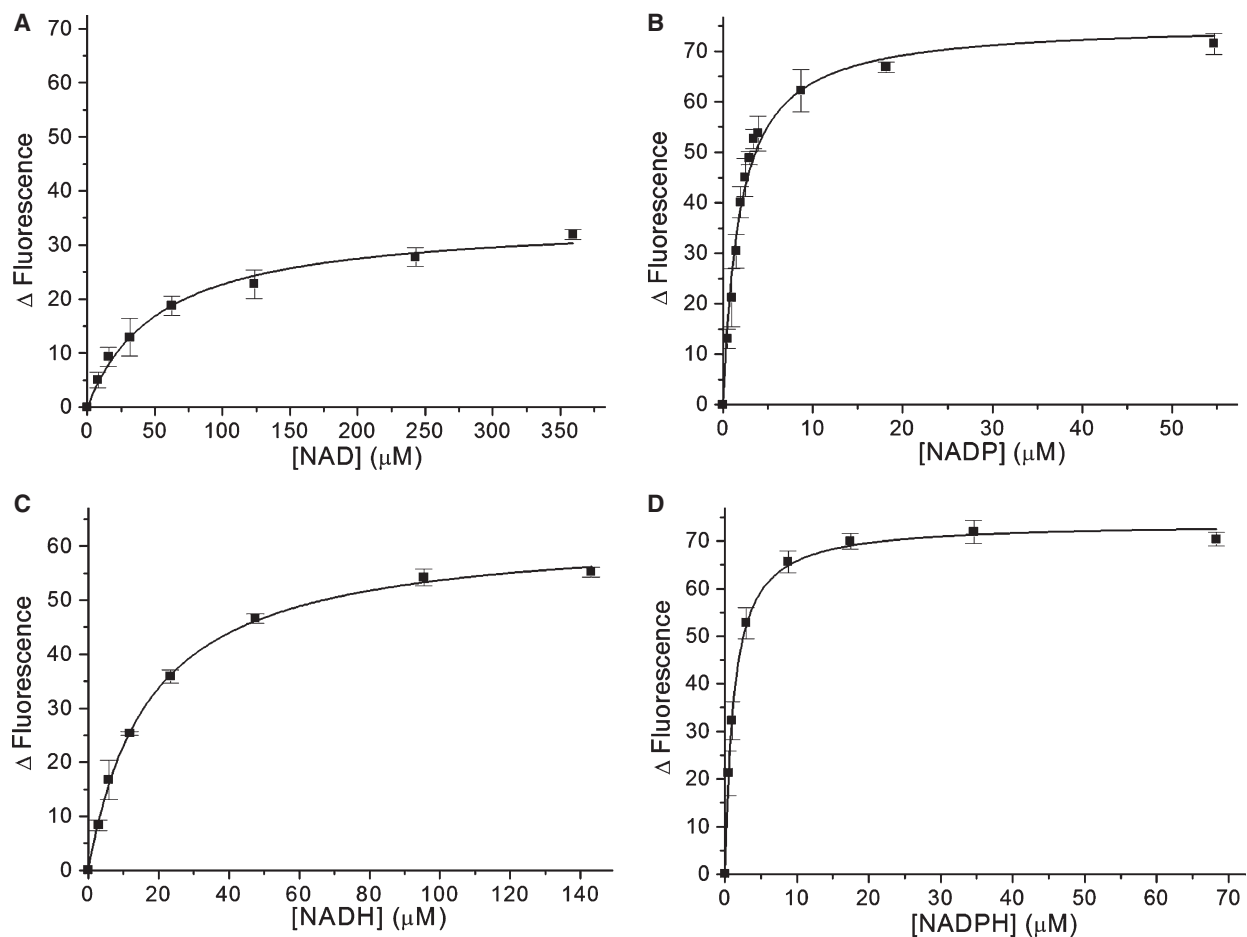


Fig. 4. Binding curves of PTDH-E175A/A176R with both of the nicotinamide cofactors in their oxidized and reduced form. In each case three fluorescence titrations were performed and the absolute value of change in emission at 340 nm (ΔF) was corrected and plotted vs. concentration. The dissociation constant (K_D) was obtained in every case (Table 3) by nonlinear least squares regression using a single binding equation as described in the Experimental procedures section.

Table 3. Overall comparison of cofactor binding and kinetic isotope effect.

Enzyme (cofactor)	Substrate K_D NADP (μM)	Product K_D NADPH (μM)	Product K_{is} NADPH (μM)	k_{cat} (min^{-1})	^{15}V KIE
WT (NAD)	11.3 ± 0.8	29 ± 5	$233 \pm 15^{\text{a}}$	$176 \pm 8^{\text{b}}$	$2.1 \pm 0.1^{\text{c}}$
E175A/A176R (NAD)	53 ± 7	17.4 ± 0.8	ND ^d	236.4 ± 0.5	2.21 ± 0.03
E175A/A176R (NADP)	1.9 ± 0.2	1.22 ± 0.06	1.2 ± 0.2	114 ± 33	1.7 ± 0.1

Previously reported by ^a [21]; ^b [23]; ^c [36]. ^d Not determined.

Table 4. Binding constants of cofactors with and without sulfite to determine order.

Enzyme (cofactor)	K_D sulfite	K_D sulfite (μM) with NADP	K_D NADP (μM)	K_D NADP (μM) with sulfite
WT (NAD)	No significant	0.76 ± 0.04	11.3 ± 0.8	0.61 ± 0.03
E175A/A176R (NAD)	binding	1.00 ± 0.05	53 ± 7	1.29 ± 0.08
E175A/A176R (NADP)	observed ^a	0.60 ± 0.06	1.9 ± 0.2	$< 0.5^{\text{b}}$

^a See text. ^b K_D below determination limits of this method.

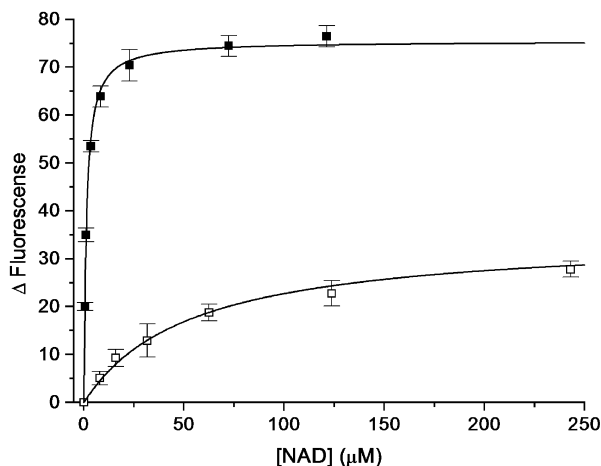


Fig. 5. Binding of NAD to PTDH-E175A/A176R in the presence of 0.2 mM of the competitive inhibitor sulfite (■) and in the absence of sulfite (□).

KIE on V_{\max} which is 2.21 with NAD, but only 1.7 with NADP. Thus, the K_{IS} for NADPH was determined as described in Experimental procedures (Fig. 6). The data could be accurately fit with the competitive inhibition model showing a large change in the slope and not a significant change in the intercepts. The K_{IS} obtained from this fit is $1.2 \pm 0.2 \mu\text{M}$, which is in good agreement with the K_D determined for NADPH ($1.22 \mu\text{M}$) and lower than the K_m of NADP

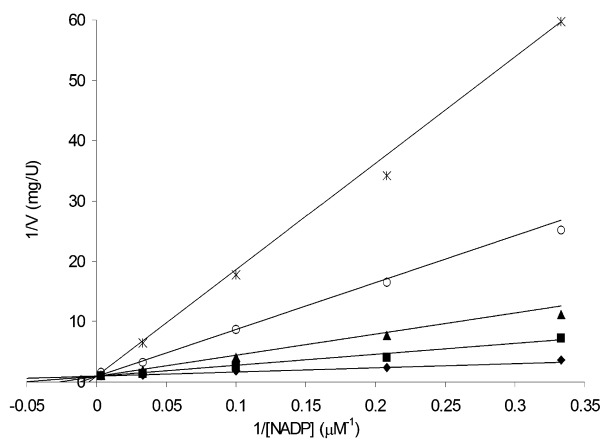


Fig. 6. Initial velocity patterns for the oxidation of phosphite with NADP in the presence of NADPH. Each data point represents the average of two identical assays initiated by addition of $2 \mu\text{g}$ PTDH-E175A/A176R. The phosphite concentration was held constant at $28 \mu\text{M}$, while the NADP concentration was varied from 3 to $300 \mu\text{M}$. The reaction product NADPH was included in the assay mixture at the concentration of 0 (◆), 2 (■), 5 (▲), 12.5 (○), and 30 (*) μM . The data was fit with the competitive inhibition model, which was used to determine the inhibition constant (K_{IS}) for NADPH.

($3.5 \mu\text{M}$). Thus, product inhibition might potentially slow NADPH regeneration in a biocatalytic regenerative process.

Use of PTDH-E175A/A176R for cofactor regeneration

The impetus for creating a PTDH that could utilize NADP efficiently was to couple it to the vast array of biosynthetic NADPH utilizing enzymes. One such enzyme is the recently characterized xylose reductase (XR) from *Neurospora crassa* [33], which catalyzes the NADPH dependent conversion of xylose into xylitol with very high catalytic efficiency. As xylitol production from xylose is commercially significant and has previously been coupled to *in situ* cofactor regeneration [51–53] we chose this process to compare WT PTDH, PTDH-E175A/A176R, and the commercially available NADP-specific FDH mutant. Small-scale reactions were carried out and analyzed as discussed in Experimental procedures. Figure 7 displays 500 mM xylose being converted quantitatively into xylitol within a 24-h period utilizing PTDH-E175A/A176R. The xylitol productivity was $75 \text{ g}\cdot\text{L}^{-1}\cdot\text{day}^{-1}$ with a total turnover number of 2500 for NADP. Use of the WT PTDH and the mutant FDH resulted in approximately fourfold slower reaction rates. Thus, it appears that PTDH-E175A/A176R is not significantly hindered by NADPH inhibition during regeneration, and should

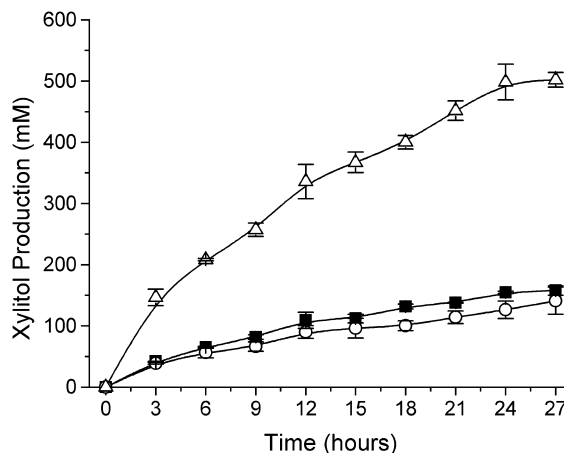


Fig. 7. NADPH regeneration coupled to production of xylitol by xylose reductase. Small-scale reactions containing xylose, xylose reductase, NADP, phosphite, and equal molar amounts of WT PTDH (○), PTDH-E175A/A176R (△), or NADP-specific formate DH (■) were compared to estimate the NADPH regeneration ability of these enzymes. PTDH-E175A/A176R permitted the biocatalytic system to progress significantly faster than either the NADP-specific FDH or the WT PTDH.

be very useful for a variety of NADPH-dependent bioconversions. Although the equilibrium value for the XR catalyzed reaction lies in favor of xylitol ($K_{\text{eq}} = 500$) [54] the primary driving force for this bioconversion comes from the PTDH catalyzed reaction ($K_{\text{eq}} = 10^{11}$ in favor of products), which allows it to drive even unfavorable reactions [22]. Another potential benefit of using the phosphite/PTDH regeneration system is that phosphite is a very low cost reductant (4.05 USD·mol⁻¹ phosphorous acid, Aldrich 2005) that is similar in price to formate (2.39 USD·mol⁻¹ formic acid, Aldrich 2005). The cost of these sacrificial reductants is insignificant compared with the overall cost for the bioconversion which resides mostly in the enzymes. Phosphate accumulation is not a problem as PTDH is not inhibited by phosphate (which is also used in the FDH system as a buffer) and phosphate can be easily removed down stream if necessary by ionic filtration or precipitation as a calcium salt. In the future, improvements on the already promising bioconversion productivity may be achieved by implementing a laboratory-scale enzyme membrane reactor.

Conclusion

In summary, the reaction catalyzed by PTDH-E175A/A176R is faster and more efficient than that by the WT PTDH with the corresponding cofactor (Table 1), but the chemical step appears to be rate determining to about the same extent as for the WT enzyme. If NADPH release indeed becomes partially rate determining, then in the presteady state time period a 'burst phase' should be observed, a prediction that is currently under investigation using stopped flow analysis. The observed isotope effect coupled with the strong thermodynamic driving force ultimately suggests that there may still be plenty of room for improvement of catalysis. Therefore, directed molecular evolution methodology is being utilized to further enhance the kinetic and stability parameters of PTDH-E175A/A176R.

Experimental procedures

Materials

Escherichia coli BL21 (DE3) and pET-15b were purchased from Novagen (Madison, WI, USA). Isopropyl- β -D-thiogalactopyranoside (IPTG), NAD, NADP, NADH, and NADPH were obtained from Sigma (St. Louis, MO, USA). Phosphorous acid, sodium sulfite and deuterium oxide were provided by Aldrich (Milwaukee, WI, USA) and sodium phosphite by Riedel-de Haën (Seelze, Germany). Sodium sulfate, sodium phosphate, xylose, xylitol, and other

required salts and reagents were purchased from either Fisher (Pittsburg, PA, USA) or Sigma-Aldrich. The POROS MC20 resin used for immobilized metal affinity chromatography (IMAC) was purchased from PerSeptive Biosystems (Framingham, MA, USA). The Millipore Amicon 8400 stirred ultrafiltration cell and corresponding YM10 membranes were purchased from Fisher. NADP-specific FDH from *Pseudomonas* sp.101 was purchased from Juelich Fine Chemicals (Juelich, Germany).

Preparation of deuterium-labeled phosphite

Deuterium-labeled phosphite was prepared according to [35,36] by heating a 1 M solution of phosphorous acid in deuterium oxide to 40 °C for 12 h. The solvent was removed on a rotary evaporator and the phosphorous acid was dissolved again in deuterium oxide, repeating the process twice to achieve complete labeling as determined by ³¹P NMR spectroscopy (500 MHz Varian, H₃PO₄ as external reference δ 0 p.p.m.). D₃PO₃ δ 5.48 p.p.m.; (t, $J_{\text{P-D}} = 103$ Hz). H₃PO₃ δ 5.75 p.p.m. (d, $J_{\text{P-H}} = 674$ Hz). Completely labeled phosphite was then lyophilized to dryness and stored in a desiccator. While the acidic form of phosphite rapidly exchanges, solutions of the dianionic form can be prepared in aqueous buffer (pH 7–8) without significant exchange over periods of weeks.

Overexpression and purification of PTDH

An overlap extension PCR-based site-directed mutagenesis method was utilized to create the double mutant E175A/A176R PTDH as previously described [23]. The N-terminal His6-Tag fusion proteins were overexpressed using *E. coli* BL21 (DE3) and purified using the IMAC purification protocol previously described [23]. For the fluorescence quenching studies, 50 mM pH 7.25 Mops buffer that was devoid of NaCl, glycerol, or dithiothreitol was used for additional desalting steps to ensure the protein and titrated ligand were in the same buffer. This protein was stored as frozen aliquots at -80 °C as concentrated as possible (≈ 50 μM dimer) without the addition of glycerol.

Protein characterization

Protein purity was assessed by SDS/PAGE [55], stained by Coomassie brilliant blue. Protein concentration was determined by the Bradford method [56] using bovine serum albumin as a standard and by absorbance using the extinction coefficient for PTDH of 30 mm⁻¹·cm⁻¹ at 280 nm.

Kinetic analysis

Initial rates were determined by monitoring the increase in absorbance, corresponding to the production of NADPH

($\epsilon_{\text{NADPH}} = 6.22 \text{ mM}^{-1}\cdot\text{cm}^{-1}$ at 340 (nm). All initial rate assays were carried out using a Varian Cary 100 Bio UV-visible spectrophotometer with the temperature of the various stock solutions and the observation cell maintained at 25 °C by a recirculating water bath. The reaction was initiated by addition of 1.8–2.5 μg of WT or PTDH-E175A/A176R. Concentrations of NAD stock solutions were determined by UV-visible spectroscopy ($\epsilon_{\text{NAD}^+} = 18 \text{ mM}^{-1}\cdot\text{cm}^{-1}$ at 260 nm). Phosphite concentrations were determined enzymatically by measuring the amount of NADH produced after all phosphite had been oxidized by WT PTDH. For kinetic isotope effect experiments, the Michaelis–Menten parameters V_{max} and K_{m} were determined by a series of assays in which six varying concentrations of NADP were used in the presence of saturating concentrations (at least 10-fold greater than the corresponding K_{m}) of either labeled (Pt-D) or unlabeled phosphite (Pt). Then the reverse experiment was carried out by varying phosphite concentration and keeping NADP saturated. Each assay was carried out at least twice in three separate experiments with the averages and associated standard deviations represented in Fig. 1. The data were then converted to turnover number (k_{cat}) and fitted with the Michaelis–Menten equation using Microcal ORIGIN 5.0 (Microcal Software, Northampton, MA, USA) nonlinear regression analysis.

For the determination of the inhibition constant of NADPH (K_{IS}), a matrix of 25 assays was carried out utilizing five varying concentrations of NADP (300, 30, 10, 4.8, and 3 μM) and five varying concentrations of NADPH (30, 12.5, 5, 2, and 0 μM) containing 28 μM phosphite. The initial rates of each assay were analyzed with a modified version of Cleland's FORTRAN program [57,58]. The K_{IS} for NADPH was obtained by fitting the data to a competitive binding model with respect to NADP, where v is the initial velocity, V is the maximum velocity, A is the concentration of NADP, K_{m} is the Michaelis–Menten constants for NADP, I is the inhibitor (NADPH) concentration, and K_{IS} is the inhibition constant (Eqn 1). All assays were performed in duplicate and the average is graphically represented in Fig. 5, the standard deviation for K_{IS} was obtained from the best-fit analysis.

$$v = VA/(K_{\text{m}}(1 + I/K_{\text{IS}}) + A) \quad (1)$$

Determination of binding constants

Fluorescence titration experiments were performed with 200 μL of 0.25 μM His6-tagged dimer of PTDH-E175A/A176R freshly diluted in 50 mM Mops buffer adjusted to a pH of 7.25. Intrinsic tryptophan fluorescence was measured with an excitation wavelength of 295 nm (2.5 nm slit width) while monitoring emission from 310 to 380 nm (2.5 nm slit width). All fluorescence measurements were taken on a Fluoromax-2 (ISA-Jobin Yvon SPEX, Edison

NJ, USA) using a 0.2 cm \times 1 cm quartz cuvette (1 cm side facing emission filter). Varying concentrations of cofactor or sulfite prepared in the same buffer were titrated into the cuvette containing the protein solution. The total sample volume was never diluted more than 7.5% over the entire titration. In the case of ordered binding experiments 0.3 mM of NAD or 0.1 mM NADP (greater than fivefold over the respective K_{D}) was added prior to titrating with sulfite. In the reverse experiments 0.2 mM sulfite was added prior to titration with NADP. All titrations were carried out at room temperature (25 °C) and in triplicate. The emission spectrum of the buffer solution was subtracted from the data, which were also corrected to account for the dilution of each addition. In the case of NADPH titrations, the large absorbance at 340 nm for the substrate coincides with the λ_{max} of emission of the protein and thus the spectra were further corrected for the inner filter effect [59]. NADP titrations were also corrected for the inner filter effect, but the low absorbance at the exciting and emitting wavelengths typically resulted in corrections of less than 5%. Binding constants were determined by plotting the corrected change in emission at the λ_{max} of 340 nm against concentration of titrant. A single binding site equation (Eqn 2) was used to fit the data with Microcal ORIGIN 5.0 (Microcal Software, Northampton, MA, USA) nonlinear regression analysis where ΔF is the observed change in fluorescence, ΔF_{max} is the maximal change in fluorescence with the given titrant, A is the concentration of the titrant, and K_{D} is the dissociation constant for the given titrant. Each experiment was performed at least three times for which the average values and standard deviation were obtained as represented in Table 4.

$$\Delta F = (\Delta F_{\text{max}}A)/(K_{\text{D}} + A) \quad (2)$$

NADPH regeneration for xylitol formation

NADPH regeneration for production of xylitol was tested on a small scale. Each sample contained 500 mM xylitol, 650 mM ammonium phosphite (ammonium formate in the case of FDH), 0.2 mM NADP, 108 μg of purified xylose reductase from *Neurospora crassa* [33], and either 154 μg of WT PTDH, 154 μg of PTDH-E175A/A176R, or 176 μg of NADP-specific FDH (4 nmol of each regenerative enzyme) and was adjusted to pH 6.9. The final volume of each reaction was 300 μL . Each reaction was started by the addition of xylose reductase, mixed and placed in a 25 °C water bath. Every 3 h, 20 μL samples were removed and immediately frozen at -80 °C. Samples were thawed directly prior to analysis, diluted 20-fold in millipure water, and injected into a Shimadzu-10A HPLC system. Xylose and xylitol were separated on an Alltech PrevailTM 5 μm Carbohydrate ES 250 \times 4.6 mm column using an isocratic elution of 49.96% water, 0.04% NH_4OH , and 50% acetonitrile at a flow rate of 0.8 $\text{mL}\cdot\text{min}^{-1}$. The samples were detected by an inline

Shimadzu ELSD-LT detector using N₂ as the carrier gas and the peak area was used to calculate conversion based on a standard curve previously prepared from authentic xylitol. Each reaction was performed and analyzed at least twice and the reported values are the average of the two measurements with the associated standard deviation.

Acknowledgements

Support for this research was provided by the NIH (GM63003) and the Biotechnology Research and Development Consortium (BRDC) (Project 2-4-121). We thank Heather Relyea for her help with ³¹P NMR experiments in the preparation of deuterated phosphite. The fluorescence experiments reported in this paper were performed at the Laboratory for Fluorescence Dynamics (LFD) at the University of Illinois at Urbana-Champaign (UIUC). The LFD is supported jointly by the National Center for Research Resources of the National Institutes of Health (PHS 5 P41-RRO3155) and UIUC.

References

- Zaks A (2001) Industrial biocatalysis. *Curr Opin Chem Biol* **5**, 130–136.
- Schmid A, Dordick JS, Hauer B, Kiener A, Wubbolts M & Witholt B (2001) Industrial biocatalysis today and tomorrow. *Nature* **409**, 258–268.
- Liese A & Filho MV (1999) Production of fine chemicals using biocatalysis. *Curr Opin Biotechnol* **10**, 595–603.
- Koeller KM & Wong CH (2001) Enzymes for chemical synthesis. *Nature* **409**, 232–240.
- Zhao H, Chockalingam K & Chen Z (2002) Directed evolution of enzymes and pathways for industrial biocatalysis. *Curr Opin Biotechnol* **13**, 104–110.
- Schoemaker HE, Mink D & Wubbolts MG (2003) Dispelling the myths – biocatalysis in industrial synthesis. *Science* **299**, 1694–1697.
- Hummel W (1999) Large-scale applications of NAD(P)-dependent oxidoreductases: recent developments. *Trends Biotechnol* **17**, 487–492.
- Zhao H & van der Donk WA (2003) Regeneration of cofactors for use in biocatalysis. *Curr Opin Biotechnol* **14**, 583–589.
- van der Donk WA & Zhao H (2003) Recent developments in pyridine nucleotide regeneration. *Curr Opin Biotechnol* **14**, 421–426.
- Chenault HK, Simon ES & Whitesides GM (1988) Cofactor regeneration for enzyme-catalysed synthesis. *Biotechnol Genet Eng Rev* **6**, 221–270.
- Chenault HK & Whitesides GM (1987) Regeneration of nicotinamide cofactors for use in organic synthesis. *Appl Biochem Biotechnol* **14**, 147–197.
- Woodyer RD, Johannes TW & Zhao H (2005) Regeneration of cofactors for enzyme biocatalysis. In *Enzyme Technology* (Pandey A, Webb C, Soccol CS & Larroche C, eds), pp. 85–103. Asiatech Publishers Inc., New Delhi, India.
- Berrios-Rivera SJ, Bennett GN & San KY (2002) Metabolic engineering of *Escherichia coli*: increase of NADH availability by overexpressing an NAD(+)-dependent formate dehydrogenase. *Metab Eng* **4**, 217–229.
- Leonida MD (2001) Redox enzymes used in chiral syntheses coupled to coenzyme regeneration. *Curr Medical Chem* **8**, 345–369.
- Woodyer R, van der Donk WA & Zhao H (2005) Optimizing a biocatalyst for improved NAD(P)H regeneration: Directed evolution of phosphite dehydrogenase. *Comb Chem High Throughput Screening* (in press).
- Wagenknecht PS, Penney JM & Hembre RT (2003) Transition-metal-catalyzed regeneration of nicotinamide coenzymes with hydrogen. *Organometallics* **22**, 1180–1182.
- Tishkov VI, Galkin AG, Marchenko GN, Egorova OA, Sheluho DV, Kulakova LB, Dementieva LA & Egorov AM (1993) Catalytic properties and stability of a *Pseudomonas* sp.101 formate dehydrogenase mutants containing Cys-255-Ser and Cys-255-Met replacements. *Biochem Biophys Res Commun* **192**, 976–981.
- Bommarius AS & Drauz K (1994) An enzymatic route to L-ornithine from arginine – activation, selectivity and stabilization of L-arginase. *Bioorg Med Chem* **2**, 617–626.
- McCoy M (2001) Making drugs with little bugs. *Chem Engineer News* **79**, 37–43.
- Carugo O & Argos P (1997) NADP-dependent enzymes. I: Conserved stereochemistry of cofactor binding. *Proteins* **28**, 10–28.
- Costas AM, White AK & Metcalf WW (2001) Purification and characterization of a novel phosphorus-oxidizing enzyme from *Pseudomonas stutzeri* WM88. *J Biol Chem* **276**, 17429–17436.
- Vrtis JM, White A, Metcalf WW & van der Donk WA (2002) Phosphite dehydrogenase, a new versatile cofactor regeneration enzyme. *Angew Chem Int Ed Engl* **41**, 3257–3259.
- Woodyer R, van der Donk WA & Zhao H (2003) Relaxing the nicotinamide cofactor specificity of phosphite dehydrogenase by rational design. *Biochemistry* **42**, 11604–11614.
- Nishiyama M, Birktoft JJ & Beppu T (1993) Alteration of coenzyme specificity of malate dehydrogenase from *Thermus flavus* by site-directed mutagenesis. *J Biol Chem* **268**, 4656–4660.
- Wiegert T, Sahn H & Sprenger GA (1997) The substitution of a single amino acid residue (Ser-116?Asp) alters NADP-containing glucose-fructose oxidoreductase of *Zymomonas mobilis* into a glucose dehydrogenase

- with dual coenzyme specificity. *J Biol Chem* **272**, 13126–13133.
- 26 Steen IH, Lien T, Madsen MS & Birkeland NK (2002) Identification of cofactor discrimination sites in NAD-isocitrate dehydrogenase from *Pyrococcus furiosus*. *Arch Microbiol* **178**, 297–300.
- 27 Bocanegra JA, Scrutton NS & Perham RN (1993) Creation of an NADP-dependent pyruvate dehydrogenase multienzyme complex by protein engineering. *Biochemistry* **32**, 2737–2740.
- 28 Zhang L, Ahvazi B, Szittner R, Vrieland A & Meighen E (1999) Change of nucleotide specificity and enhancement of catalytic efficiency in single point mutants of *Vibrio harveyi* aldehyde dehydrogenase. *Biochemistry* **38**, 11440–11447.
- 29 Schepens I, Johansson K, Decottignies P, Gillibert M, Hirasawa M, Knaff DB & Miginiac-Maslow M (2000) Inhibition of the thioredoxin-dependent activation of the NADP-malate dehydrogenase and cofactor specificity. *J Biol Chem* **275**, 20996–21001.
- 30 Nakanishi M, Matsuura K, Kaibe H, Tanaka N, Nonaka T, Mitsui Y & Hara A (1997) Switch of coenzyme specificity of mouse lung carbonyl reductase by substitution of threonine 38 with aspartic acid. *J Biol Chem* **272**, 2218–2222.
- 31 Danielson UH, Jiang F, Hansson LO & Mannervik B (1999) Probing the kinetic mechanism and coenzyme specificity of glutathione reductase from the cyanobacterium *Anabaena* PCC 7120 by redesign of the pyridine-nucleotide-binding site. *Biochemistry* **38**, 9254–9263.
- 32 Galkin A, Kulakova L, Ohshima T, Esaki N & Soda K (1997) Construction of a new leucine dehydrogenase with preferred specificity for NADP⁺ by site-directed mutagenesis of the strictly NAD⁺-specific enzyme. *Protein Eng* **10**, 687–690.
- 33 Woodyer R, Simurdiak M, van der Donk WA & Zhao H (2005) Heterologous expression, purification and characterization of a highly active xylose reductase from *Neurospora crassa*. *Appl Environ Microbiol* **71**, 1642–1647.
- 34 Relyea H & van der Donk WA (2005) Mechanism and applications of phosphite dehydrogenase. *Bioorg Chem* **33**, 171–189.
- 35 Martin R (1959) The rate of exchange of the phosphorus bonded hydrogen in phosphorous acid. *J Am Chem Soc* **81**, 1574–1576.
- 36 Vrtis JM, White AK, Metcalf WW & van der Donk WA (2001) Phosphite dehydrogenase: an unusual phosphoryl transfer reaction. *J Am Chem Soc* **123**, 2672–2673.
- 37 Northrop DB (1977) Determining the absolute magnitude of hydrogen isotope effects. In *Isotope Effects on Enzyme-Catalyzed Reaction* (Cleland, W W, O'Leary, M H & Northrop, D B, eds), pp. 122–152. University Park Press, Baltimore, MD.
- 38 Duggleby RG & Northrop DB (1989) The expression of kinetic isotope effects during the time course of enzyme catalyzed reactions. *Bioorg Chem* **17**, 177–193.
- 39 Cleland WW (1977) Determining the chemical mechanisms of enzyme-catalyzed reactions by kinetic studies. *Adv Enzymol Relat Areas Mol Biol* **45**, 273–387.
- 40 Nidetzky B, Helmer H, Klimacek M, Lunzer R & Mayer G (2003) Characterization of recombinant xylytol dehydrogenase from *Galactocandida mastotermitis* expressed in *Escherichia coli*. *Chem Biol Interact* **143–144**, 533–542.
- 41 Dunning Hotopp JC, Auchtung TA, Hogan DA & Hausinger RP (2003) Intrinsic tryptophan fluorescence as a probe of metal and alpha-ketoglutarate binding to TfdA, a mononuclear non-heme iron dioxygenase. *J Inorg Biochem* **93**, 66–70.
- 42 Espinosa V, Kettlun AM, Zanocco A, Cardemil E & Valenzuela MA (2003) Differences in nucleotide-binding site of isoapyrases deduced from tryptophan fluorescence. *Phytochemistry* **63**, 7–14.
- 43 Garnier C, Lafitte D, Tsvetkov PO, Barbier P, Leclerc-Devin J, Millot JM, Briand C, Makarov AA, Catelli MG & Peyrot V (2002) Binding of ATP to heat shock protein 90: evidence for an ATP-binding site in the C-terminal domain. *J Biol Chem* **277**, 12208–12214.
- 44 Hegde SS, Dam TK, Brewer CF & Blanchard JS (2002) Thermodynamics of aminoglycoside and acyl-coenzyme A binding to the *Salmonella enterica* AAC (6')-Iy aminoglycoside N-acetyltransferase. *Biochemistry* **41**, 7519–7527.
- 45 Liu J, Tian JN, Zhang J, Hu Z & Chen X (2003) Interaction of magnolol with bovine serum albumin: a fluorescence-quenching study. *Anal Bioanal Chem* **376**, 864–867.
- 46 Nagase T, Nakata E, Shinkai S & Hamachi I (2003) Construction of artificial signal transducers on a lectin surface by post-photoaffinity-labeling modification for fluorescent saccharide biosensors. *Chemistry* **9**, 3660–3669.
- 47 Serov AE, Popova AS, Fedorchuk VV & Tishkov VI (2002) Engineering of coenzyme specificity of formate dehydrogenase from *Saccharomyces cerevisiae*. *Biochem J* **367**, 841–847.
- 48 Xia X, Lin JT & Kinne RK (2003) Binding of phlorizin to the isolated C-terminal extramembranous loop of the Na⁺/glucose cotransporter assessed by intrinsic tryptophan fluorescence. *Biochemistry* **42**, 6115–6120.
- 49 Zang H & Gates KS (2000) DNA binding and alkylation by the 'left half' of azinomycin B. *Biochemistry* **39**, 14968–14975.
- 50 Relyea HA, Vrtis JM, Woodyer R, Rimkus SA & van der Donk WA (2005) Inhibition and pH dependence of phosphite dehydrogenase. *Biochemistry* **44**, 6640–6649.

- 51 Kitpreechavanich V, Nishio N, Hayashi M & Nagai S (1985) Regeneration and retention of NADP(H) for xylitol production in an ionized membrane reactor. *Biotechnol Lett* **7**, 657–662.
- 52 Nidetzky B, Schmidt B, Neuhauser W, Haltrich D & Kulbe KD (1994) Application of charged ultrafiltration membranes in continuous, enzyme-catalyzed processes with coenzyme regeneration. In *Separations for Biotechnology* (Pyle, D L, ed.), pp. 351–357. Royal Society of Chemistry, London.
- 53 Nidetzky B, Neuhauser W, Haltrich D & Kulbe KD (1996) Continuous enzymatic production of xylitol with simultaneous coenzyme regeneration in a charged membrane reactor. *Biotechnol Bioeng* **52**, 387–396.
- 54 Nidetzky B, Klimacek M & Mayr P (2001) Transient-state and steady-state kinetic studies of the mechanism of NADH-dependent aldehyde reduction catalyzed by xylose reductase from the yeast *Candida tenuis*. *Biochemistry* **40**, 10371–10381.
- 55 Laemmli UK (1970) Cleavage of structural proteins during the assembly of the head of bacteriophage T4. *Nature* **227**, 680–685.
- 56 Bradford MM (1976) A rapid and sensitive method for the quantitation of microgram quantities of protein utilizing the principle of protein-dye binding. *Anal Biochem* **72**, 248–254.
- 57 Robertson JG (1979) *Kineticsyst*. In *Intellikinetics*. State College, PA.
- 58 Cleland WW (1979) Statistical analysis of enzyme kinetic data. *Methods Enzymol* **63**, 103–138.
- 59 Lakowics JR (1999) *Principles of Fluorescence Spectroscopy*, 2nd edn. Kluwer Academic/Plenum, New York.